Regimes of direct contact condensation of steam injected into water

Anka de With[a,*], Raj K. Calay[a], Arne E. Holdø[b] and Govert de With[c]

[a]Fluid Mechanics Research Group, University of Hertfordshire, College Lane, Hatfield, AL10 9AB, UK
Tel.:+44 1707 284124; Fax.:+44 1707 285086
[b]Faculty of Engineering and Computing, Coventry University, Priory Street, Coventry CV1 5FB
[c]Lafarge Roofing Technical Centers Ltd, Sussex Manor Business Park, Gatwick Road, Crawley, RH10 9NZ, UK
Tel.:+44 1293 596309; Fax.:+44 1293 596427

ABSTRACT

Direct contact condensation of steam injected into water is a special mode of condensation where condensation occurs on the interface between steam and water. Crucial in the modelling of direct contact condensation is the behaviour of the injected steam, commonly termed as a regime. Depending on the environmental conditions, steam injected into water appears in different regimes. These are observed in different geometrical appearances of the injected steam and are ranging from steam being condensed in the injector to bubbles and jets of steam formed in water.

The two dimensional regime maps and models presently available are able to predict different condensation behaviour for limited range of flow conditions. In this paper a new three-dimensional condensation regime diagram is presented. The diagram is capable of predicting regimes for a wide range of flow conditions as well as different sizes of steam injector. Furthermore, expected penetration distance of steam injected into water, which is also crucial in modelling of the process, is presented for different flow conditions in the form of a new two-dimensional steam plume length diagram.

Keywords: steam; direct contact condensation; regimes; regime map; plume length

NOMENCLATURE

B	condensation potential
c_p	specific heat at constant pressure
D	diameter of steam injector
G	steam flow rate
h_{fg}	latent heat
L	plume length

*Corresponding author. E-mail addresses: a.de-with@herts.ac.uk (Anka de With), r.k.calay@herts.ac.uk (Raj K. Calay), Erik.Holdo@coventry.ac.uk (Arne E. Holdø), govert.de.with@lafargeroofing.com (Govert de With).

R injector radius
Re steam Reynolds number
T temperature
ΔT temperature of water subcooling
η viscosity

Subscript
m mean value
s steam
w water
0 at the injector

1. INTRODUCTION

A condensation of steam injected into water is an example of multiphase flows. Multiphase flows are the most common flows of fluids in nature and they appear in many industrial devices. Some examples of multiphase flows are boiling and condensing liquids, the drifting of clouds in the atmosphere and liquid sprays. The frequent appearance and industrial significance of multiphase flows has resulted in intensive investigation of the subject, both experimentally and theoretically. Studies by Guha [1], Whalley [2], Hetsroni [3] and Drew and Passman [4] have contributed significantly to our present understanding of multi-phase flows and their work has formed the basis for most of the multi-phase computer models. Despite these substantial developments in the field of multi-phase flows, accurate modelling remains out-of-reach when the phase transition is the dominant flow feature, as seen in condensation.

Direct Contact Condensation (DCC) of steam in water occurs when steam is introduced into water. It is a phenomenon of high importance used in devices for nuclear, chemical, and marine industry. However, at present there is still limited knowledge on the subject of DCC. When DCC takes place there is a transfer of water vapour from gas into liquid form, causing heat, momentum and energy transfer. During DCC the transfer of mass, energy and momentum is subject to the local characteristics of the condensation process; hence, the performance of such engineering devices depends strongly on the local condensation characteristics and therefore detailed knowledge of the process is required to optimize the performance. The behaviour of DCC is investigated in various experimental studies [5]-[11] and while this has resulted in a substantial increase in experimental data, a generic understanding of condensation of steam in water is still very limited [12]-[15]. Existing models for predicting the performance of devices which involve DCC [16]-[18] simplify the condensation process and use empirical correlations in their model. Consequently, these empirical correlations and model assumptions limit the capability of these models.

The most descriptive information about the steam plume behaviour is found in summary form in a regime map. This map is a graph describing the appearance of different regimes at specific conditions in terms of their geometric appearances and dynamic features. Various regime maps have been published in literature [6], [7], [9], [19]-[21] which show the occurrence of different regimes, depending on the steam inflow rate and the temperature of water subcooling. These two-dimensional maps were obtained during experiments performed at various environmental conditions. These are inflow conditions, injector geometry and the water flow conditions. The two-dimensional maps published by different researchers show similar features of the process. However, due to differences in injector geometry these features were observed under different inflow conditions. This leads to the conclusion, that the condensation behaviour is case specific and the environmental

conditions during the experiment affect the occurrence of the regime. Therefore, a single two-dimensional regime map should not serve as a basis of identifying the DCC regimes.

Another important feature of the DCC process is the penetration distance of steam into water also known as steam plume length. In the literature a number of empirical correlations for a dimensionless steam plume length is proposed [5], [11], [14], [22]. These correlations present a ratio between the steam plume length and the diameter of the injector as a function of the water subcooling and the steam inflow rate. The error between these correlations and the corresponding experimental data is reported to be in the range of 20% to 35%. However, the error only relates to the experimental data, which has formed the basis for the proposed correlations. If the correlations are applied to a set of flow conditions well beyond the original experimental data the plume length is predicted poorly and no longer valid.

Due to the importance of the steam plume length in modelling of the DCC process, separate correlations reported in literature were used to predict the length during calculations. This resulted in a poor prediction of the flow behaviour. Consequently, there is a need for more generalised prediction of the steam plume length valid across a range of inflow conditions.

In this paper a three-dimensional condensation regime diagram and a two-dimensional steam plume length diagram are presented. For a wide range of flow conditions, these are capable of predicting the behaviour of condensing steam, the regime, and the length of a plume, the penetration distance of steam into water. They were constructed from experimental data available in literature.

2. DIRECT CONTACT CONDENSATION OF STEAM INJECTED INTO WATER

The DCC of steam injected into water is a complicated process, because it appears in different regimes, depending on the environmental conditions, and it involves different regions of the process.

Independent of the condensation regime, the process of DCC of steam injected into water consists of four different regions: a steam plume, the interface between steam and water, the hot water layer and the surrounding water. Figure 1 shows a photograph of the DCC process with added schematic picture of DCC regions.

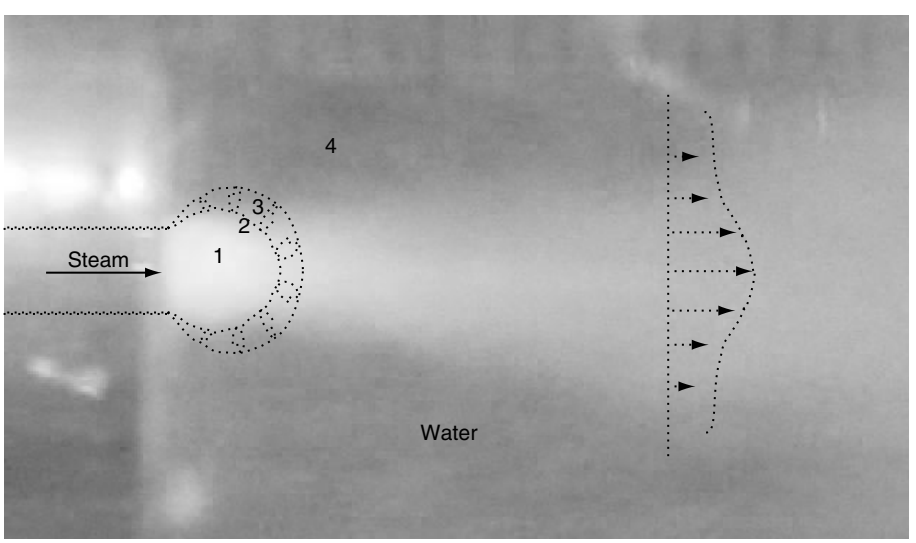

Figure 1 Photograph of the DCC taken during the experiments for a ballast water treatment system with added schematic picture of the process, showing the different regions of DCC of steam injected into water: steam plume (1), interface (2), hot water layer (3) and surrounding water (4).

The first region consists of pure steam and is called the steam plume. The plume's outer surface is the interface where condensation takes place. Surrounding the interface is a hot water layer which contains of steam bubbles and is characterized by an increase in water temperature The hot water layer is surrounded by surrounding water. A two-phase jet is formed in the surrounding water down-stream of the plume. The exact behaviour and the precise appearance of each region will differ depending on the regime. Nevertheless, each region is always present when there is a condensation of steam into water. A more detailed description of the DCC regions can be found in the work published by Petrovic-de With *et al*. [23].

2.1. REGIMES OF DCC

The shape of the steam plume is predominantly dependent on the inflow conditions. These include steam inflow rate and water subcooling temperature. Steam inflow rate (G_0) is defined as a ratio between mass flux of steam and the steam injector exit area. The water subcooling is the temperature difference between steam and water ($\Delta T = T_s - T_w$). A range of steam plume shapes can be observed during experimental observations. The dynamic behaviour and the geometrical appearance of the steam plume can be subdivided in three main regimes:

- Chugging regime
- Jetting regime
- Bubbling regime

Chugging Regime

The chugging regime is characterised by a flat or curved shape of steam plume located in the injector or its vicinity, and the steam plume size is close to the injector's cross-sectional area. Figure 2 shows a possible cycle of a chugging regime.

The chugging regime occurs at steam inflow rates up to $80 kg/(m^2 s)$, depending on the surrounding water temperature and steam injector diameter (D). The location of the steam plume in the injector may vary continuously, moving from the outer edge of the injector into the injector and backwards [6]. Chugging occurs because the steam inflow rate is smaller than the condensation rate which causes suction of surrounding water into the steam injector.

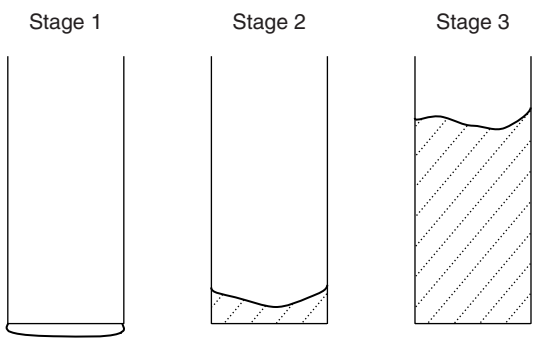

Figure 2 Chugging regime cycle from Chan & Lee [6]. The regime was observed with water subcooling of 66°*C*. The shaded area represents water. Steam is injected vertically downwards.

If chugging occurs inside the injector in a pulsating manner, the process is called interfacial condensation oscillation. For this type of condensation the steam inflow rate is normally smaller than $5kg/(m^2s)$.

Jetting Regime

For steam inflow rates higher than about $100kg/(m^2s)$, steam forms a plume which holds approximately constant size and shape. This type of condensation is called the jetting regime. Jetting consists of three main plume shapes which include: conical, ellipsoidal and divergent shape (Figure 3).

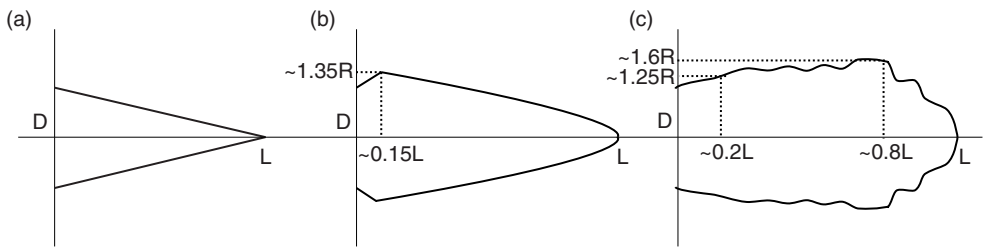

Figure 3 Jetting regime plume shapes observed by Chun *et al.* [14]. (a) Conical plume, $\Delta T = 76.7°C$, $G_0 = 286kg/(m^2s)$, $D = 10.85mm$, $L = 20mm$, (b) Ellipsoidal plume, $\Delta T = 58.5°C$, $G_0 = 312kg/(m^2s)$, $D = 7.65mm$, $L = 26mm$, (c) Divergent plume, $\Delta T = 27.1°C$, $G_0 = 530kg/(m^2s)$, $D = 7.65mm$, $L = 34mm$. Steam injection is to the right.

For some inflow conditions close to the bubbling regime, the plume can also take a hemispherical shape. The length of the steam plume (L) in the jetting regime can vary from one millimetre to more than fifteen centimetres. If the condensation occurs in a conical or ellipsoidal jetting regime, the plume will take a regular shape with a smooth surface (Figure 3 (a), (b)). For water temperatures higher than $70°C$ to $80°C$, the plume will take an irregular divergent shape (Figure 3 (c)). This regime is named divergent jetting. The length of a divergent plume is usually bigger than two centimetres.

Bubbling Regime

For steam inflow rates between chugging and jetting, bubbling occurs. Here, injected steam generates a regular or an irregular bubble at the edge of the injector. The generated bubble grows and when a maximum size of the bubble is reached, the whole or a part of the bubble is detached from the injector. The remaining part of the original bubble starts to grow until a maximum bubble size is reached [24]. In certain cases there is a collapse of the original bubble after detachment. Detached parts of the bubble are dragged away from the steam injector and continue to condense, generating a trace of smaller steam bubbles in the downstream flow [19]. Figure 4 shows a possible cycle of a bubbling regime of DCC.

Figure 4 Bubbling regime cycle observed by Simpson & Chan [24]. $\Delta T = 37°C$, $G_0 = 305.5 kg/(m^2 s)$, $D = 0.635$cm. Steam is injected vertically downwards.

3. THREE-DIMENSIONAL CONDENSATION REGIME DIAGRAM FOR DCC

The regime maps from literature show only limited accuracy. A comparison of the two-dimensional regime maps showed that all maps contain similar features. However, distinct variations are seen when comparing the regime maps based on different injector diameters For this reason a three-dimensional regime diagram is needed and has therefore been developed from a large number of independent studies published during the last three decades [5]-[8], [10], [11], [14], [19]-[21], [24]. The traditional dependencies of steam mass inflow rate (G_0) and water subcooling ($\Delta T = T_s - T_w$) are used in the three-dimensional diagram. Based on the above analysis the injector diameter (D) is selected as a third dependency. Other selections of dependency have been studied but provided very poor correlation.

All gathered data was analysed in order to identify different reported regimes. Fifteen different regimes were identified, all reported at slightly different flow conditions. For low temperature subcooling (ΔT approximately $10°C$ or less) no condensation was detected. Under these conditions, the temperature difference between steam and surrounding water is too small for the steam to condense before it escapes from the water. At high steam inflow rates ($G_0 > 300 kg/(m^2 s)$) and small temperature differences ($\Delta T < 35°C$) divergent jetting was reported. At similar steam inflow rates, but with medium to high water subcooling ($\Delta T > 35°C$) ellipsoidal jetting was reported. Conical jetting was reported at medium steam inflow rates ($120 kg/(m^2 s) < G_0 < 300 kg/(m^2 s)$) across a range of temperature differences. At small steam inflow rates ($2 kg/(m^2 s) < G_0 < 60 kg/(m^2 s)$) and temperature differences above $20°C$ a series of different chugging regimes was reported. These are internal chugging, small chugging, external chugging with detached bubbles and external chugging with encapsulating bubbles. They were reported at slightly different conditions. Furthermore, some researchers reported only some of the chugging regimes. At very small steam inflow

rates ($G_0 < 2kg/(m^2s)$) interfacial condensation oscillation was reported. Various forms of bubbling regimes were reported for conditions between the chugging regime and the conical jetting regime ($60kg/(m^2s) < G_0 < 120kg/(m^2s)$), and for conditions between the chugging regime and no condensation area ($5°C < \Delta T < 20°C$ at $1kg/(m^2s) < G_0 < 60kg/(m^2s)$). A range of different bubbling regimes were reported and included: oscillatory bubbling, ellipsoidal oscillatory bubbling, low frequency bubbling, high frequency bubbling, bubbling condensation oscillation and condensation oscillation.

For a clearer description of condensation, the data was rationalised. All different chugging regimes were grouped together in one regime and similarly also all bubbling regimes were grouped into one regime. The jetting regimes cover a large range of flow conditions and give important information about the steam plume shape; hence, the jetting regime was subdivided into three jetting regimes. As a result the regime data contains in a total of seven different regimes. A summary of the various regimes is presented in the Table 1.

Regime	$\mathbf{G_0}\left[\frac{kg}{m^2 s}\right]$	ΔT [°C]
no condensation		≤10
interfacial condensation oscillation	< 2	
chugging	ε (2,60)	>20
bubbling	ε (60,120)	ε (10,90)
	ε (1,60)	ε (5,20)
conical jetting	ε (120,300)	ε (20,90)
ellipsoidal jetting	>300	>35
divergent jetting	>30	<35

The three-dimensional condensation regime diagram was created from the three-dimensional surfaces representing the outer borders of the condensation regime. All surfaces were placed in a single graph to form a new Three-Dimensional Condensation Regime (3DCR) diagram for DCC of steam injected into stagnant water (Figure 5).

The 3DCR diagram (Figure 5) presents areas of different regimes for different steam inflow rates in the range from $0kg/(m^2s)$ to $1500kg/(m^2s)$, for steam injector diameter sizes between $0.00135m$ to $0.5m$ and for water subcooling. Seven main different regimes reported in the literature. Depending on the diameter of the steam injector, conditions at which regimes are reported vary and are in the ranges presented in this table. ranging from $0°C$ to $90°C$. For water subcooling between 90 and $100°C$ data was not available. To ensure sufficient accuracy, the diagram is constructed such that areas with insufficient data remain white.

The diagram clearly shows areas of different jetting regimes: conical jetting, ellipsoidal jetting and divergent jetting. Jetting regimes cover most of the 3DCR diagram and they appear at steam inflow rates around $200kg/(m^2s)$ and extend to high steam inflow rates. In the jetting area it can be seen that the divergent jetting appears above the no-condensation area and covers a section of the jetting area that ranges from approximately $10°C$ to $25°C$ water subcooling, depending on a steam injector diameter. Above the divergent jetting area, an ellipsoidal jetting area can be observed. It expands to high water subcooling at steam inflow rates higher than $1000kg/(m^2s)$.

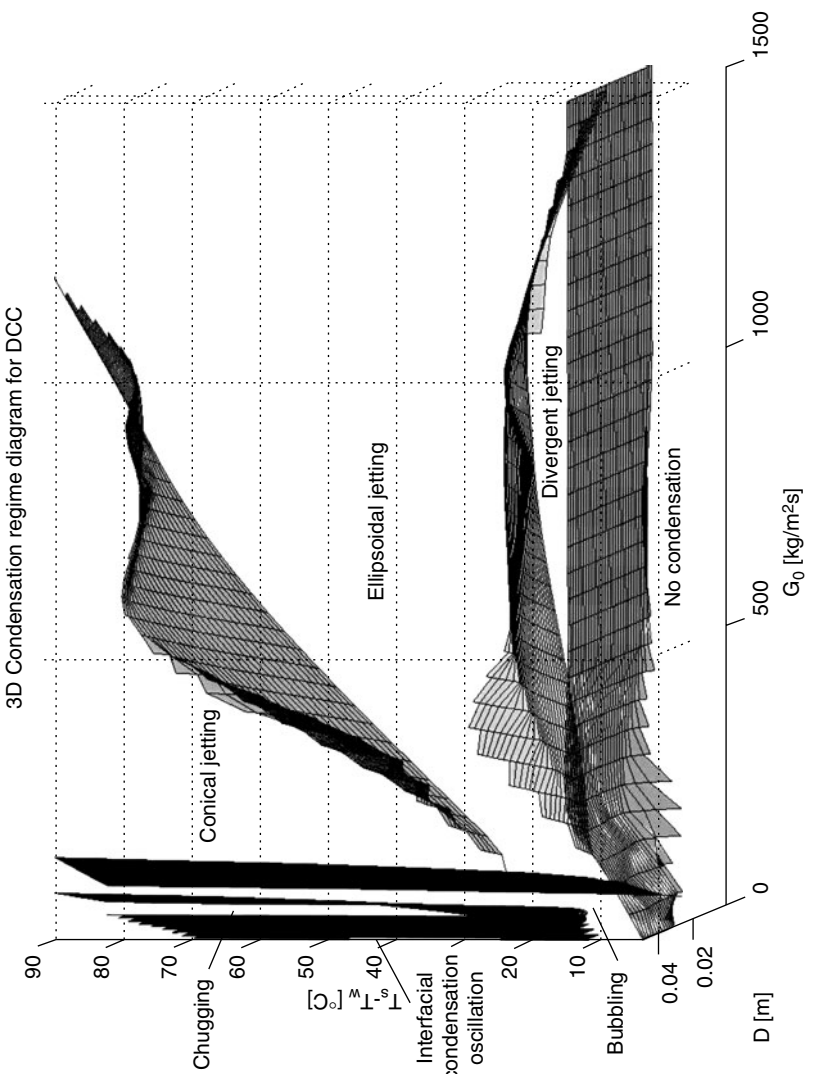

Figure 5 New 3DCR diagram. Three different jetting regimes are clearly seen on the diagram. At small steam inflow rates, bubbling, chugging and interfacial condensation oscillation can be identified.

At lower steam inflow rates, this area is diagonally cut with an area of conical jetting, which occurs at a water subcooling around 25°C at 200$kg/(m^2s)$ and expands to 90ºC at 200$kg/(m^2s)$. For steam inflow rates smaller than 200$kg/(m^2s)$ bubbling, chugging and interfacial condensation oscillation occur. The diagram shows that for very small steam inflow rates up to 2$kg/(m^2s)$ interfacial condensation oscillation ranges from 15ºC to 60ºC of water subcooling. The chugging regime starts when the water subcooling is 20°C and extends to 90°C and covers an area of the 3DCR diagram up to a steam inflow rate of 50$kg/(m^2s)$. With lower water subcooling a bubbling regime is observed. For steam inflow rates between 50$kg/(m^2s)$ and 120$kg/(m^2s)$ a bubbling regime occurs with water subcooling up to 90°C.

The 3DCR diagram was validated using data about regimes which was not used during its creation. Validation showed that the new 3DCR diagram is valid for steam inflow rates in the jetting regime and it can also be extended into a 'white' area of flow conditions. More experiments are needed to validate the diagram in the chugging and bubbling regimes. However, validation showed, that there is a general agreement between the new 3DCR diagram and the data. A detailed validation of the diagram can be found in [23].

4. TWO-DIMENSIONAL STEAM PLUME LENGTH DIAGRAM FOR DCC

In addition to the precise nature of the condensation regime, another important feature of DCC of steam into water is the length of a steam plume. In order to model DCC of steam in water the length of the steam plume is needed for a series of flow conditions of the process. However, the length of a steam plume depends on the flow conditions of the process and is therefore difficult to predict.

Until now, researchers have performed experiments where the steam plume length was measured [5], [8], [10], [11], [14]. The data was used to derive empirical correlations, predicting the dimensionless steam plume length as a function of condensation potential ($B = (c_p/h_{fg})\,\Delta T$) and dimensionless steam mass inflow rate (G_0/G_m). The constant G_m was chosen by Kerney *et al*. [5] to normalize the data to 275$kg/(m^2s)$. Unfortunately, these correlations are only valid for a narrow range of flow conditions. Therefore, there is a need for a more general correlation, capable of predicting plume lengths for a wide range of flow conditions.

In this study all the data for steam plume length available in literature was collected and used to construct the prediction for a steam plume length. All collected data was plotted on single graphs in an attempt to understand the underlying trends. First, the dimensionless steam plume length data was plotted in a graph using condensation potential B and dimensionless steam mass inflow rate G_0/G_m as axes. This method of plotting has been used by other researchers to obtain their semi-empirical correlations. Therefore, if their correlations are generally valid, the generated graph should deliver a smooth, organised distribution of data. However, the results show only limited structure and no clear defined trends.

A much more coherent plot of the experimental data was found when the graph presenting the steam plume length (L) as a function of steam Reynolds number (Re) and condensation potential (B) was generated. In addition to physical parameters, known to affect the process of DCC, the Reynolds number ($Re = DG_0/\eta$) was chosen as one of the dependencies. The Reynolds number is directly related to the inertia of injected steam and hence it should be related to the penetration length of the steam. The generated plot showed that the largest steam plume length occurs at high Reynolds numbers and low condensation potentials. The smallest lengths occur at low Reynolds numbers for all condensation potentials.

The steam plume length data as a function of Reynolds number and condensation potential was used to develop a two-dimensional steam plume length diagram. The diagram was produced

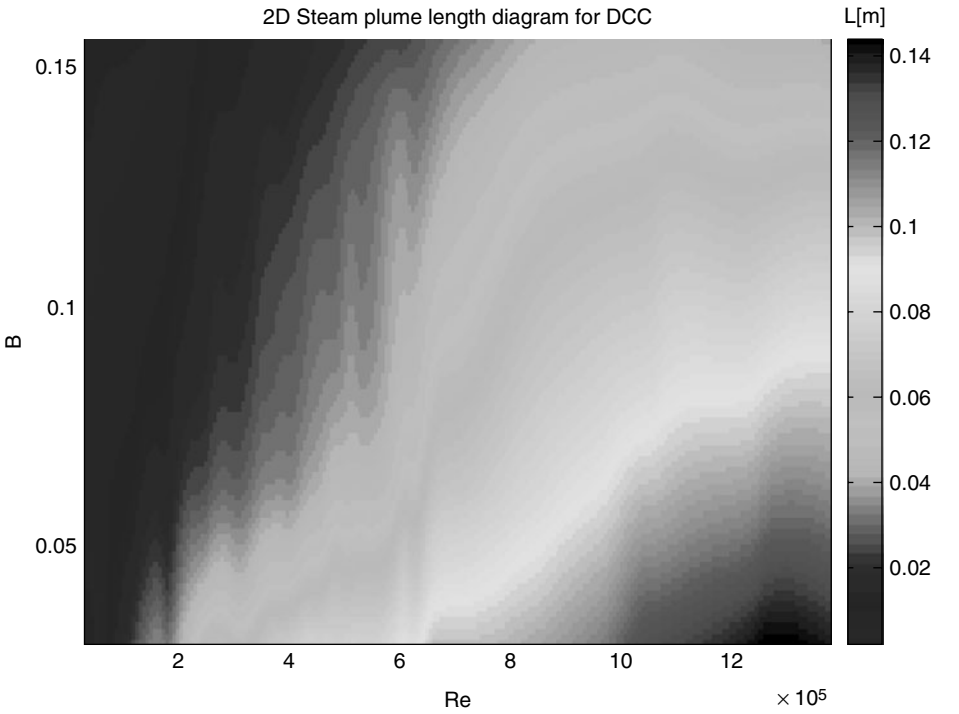

Figure 6 New 2DSPL diagram for DCC. Colours indicate predicted length of the steam plume in metres. The longest plumes are to be expected at high Reynolds numbers and low condensation potentials; short plumes at low Reynolds numbers.

through interpolation using existing data. The developed Two-Dimensional Steam Plume Length (2DSPL) diagram is given in Figure 6. The diagram shows the length of the steam plume in metres ($L[m]$) in relation to the steam Reynolds number (Re) in the range between 0.24×10^5 and 13.74×10^5, and the condensation potential (B) in the range between 0.029 and 0.155. Different colours on the diagram represent the length of the steam plume in metres.

The new 2DSPL diagram (Figure 6) shows that steam develops long plumes when injected at high Reynolds numbers and short plumes at low Reynolds numbers. Furthermore, the longest plumes are to be expected at high Reynolds numbers and low condensation potentials. This is in accordance with the physics of the process which suggests that the steam plume length is related to the condensation rate of steam and to the inertia of injected steam. In more detail, the steam plume extends with a higher inertia of the steam, but shortens at a higher rate of condensation.

The validation of the 2DSPL diagram showed the error of the diagram to be 13.7%. The data used for validation has been spread over a whole range of conditions, at which the diagram is specified. The validation also showed that the 2DSPL diagram accurately predicts lengths at both high and low Reynolds numbers. The empirical correlations from the literature were derived from experiments performed at low Reynolds numbers and are not capable of predicting accurately lengths at high Reynolds numbers. To summarize, the developed two-dimensional steam plume length diagram outperforms the semiempirical correlations from the literature for a wide range of flow conditions. A detailed validation can be found in [25].

5. CONCLUSIONS

Different regimes of direct contact condensation were presented in this paper. These are chugging, bubbling and jetting regimes. The paper describes, how different regimes are developed and at which conditions they are expected.

Furthermore, the new three-dimensional condensation regime diagram for DCC of steam injected into water was presented. The 3DCR diagram was created from experimental data taken from the literature. This data was independent and published over a period of more than three decades. The diagram can predict the existence of DCC regimes satisfactory across a wide range of flow conditions and injector sizes. This is an advantage over maps in the literature, which are able to predict regimes for one injector size only. Furthermore, the developed diagram shows, that the dimension of steam injector is an important physical parameter for characterisation of the process of DCC. Until now, researchers have only identified the steam inflow rate and the water subcooling as important parameters for the characterisation.

Also presented in the paper is the new two-dimensional steam plume length diagram for DCC of steam injected into a stagnant water. The diagram can predict lengths of the steam plume satisfactory for a wide range of flow conditions. The 2DSPL diagram has been derived from experimental data given in the literature and obtained through a number of independent experiments. Study has shown, that the length of the steam plume, in relation to steam Reynolds number and condensation potential, gives better correlation than the dimensionless steam plume length as a function of steam flow rate and condensation potential, which has been used by earlier researchers.

Information about the occurrence of different regimes and the length of a steam plume at different conditions, can be obtained from the presented diagrams and used to model the process of DCC. The developed diagrams include effects of various parameters which affect the flow characteristics of the process. Hence, the diagrams give a more generalised prediction of the DCC characteristics.

REFERENCES

[1] Guha, A.: *The Fluid Mechanics of Two-Phase Vapour Droplet Flow With Application to Steam Turbines*, PhD thesis, Trinity College, University of Cambridge, UK, 1990

[2] Whalley, P.B.: *Boiling, Condensation and Gas-Liquid Flow*, Oxford University Press Inc., New York, 1987

[3] 1. Hetsroni, G.: *Handbook of Multiphase Systems*, Hemisphere Publishing Corporation, Washington, 1982

[4] Drew, D.A. & Passman, S.L.: *Theory of Multicomponent Fluids*, Springer-Verlag New York, Inc., Printed by Maple-Vail Book Manufacturing Group, York, PA, 1999

[5] P.J. Kerney, G.M. Faeth, D.R. Olson, Penetration Characteristics of a Submerged Steam Jet, *AIChE Journal*, 1972, 18(3), 548–553

[6] C.K. Chan and C.K.B. Lee, A regime map for Direct Contact Condensation, *International Journal of Multiphase Flow*, 1982, 8(1), 11–20

[7] K.S. Liang and P. Griffith, Experimental and Analytical Study of Direct Contact Condensation of Steam in Water, *Nuclear Engineering and Design*, 1994, 147, 425–435

[8] Y.S. Kim and J.W. Park, Determination of the Steam-Water Direct Contact Condensation Heat Transfer Coefficient Using Interfacial Transport Models, *Proceedings of American Nuclear Society — Thermal Hydraulics Division*, 10, 1997, 110–117

[9] D.H. Youn, K.B. Ko, Y.Y. Lee, M.H. Kim, Y.Y. Bae, J.K. Park, The Direct Contact Condensation of Steam in a Pool at Low Mass Flux, *Journal of Nuclear Science and Technology*, 2003, 40(10), 881–885

[10] Y.S. Kim, J.W. Park, C.H. Song, Investigation of the Steam-Water Direct Contact Condensation Heat Transfer Coefficient Using Interfacial Transport Models, *International Comm. Heat Mass Transfer*, 2004, 31(3), 397–408

[11] H.Y. Kim, Y.Y. Bae, C.H. Song, J.K. Park, S.M. Choi, Experimental study on stable steam condensation in quenching tank, *International Journal of Energy Research*, 2001, 25, 239–252

[12] L.D. Chen, and G.M. Faeth, Condensation of Submerged Vapor Jets in Subcooled Liquids, *Transactions of the ASME, Journal of Heat Transfer*, 1982, 104, 774–780

[13] G.P. Celata, M. Cumo, G.E. Farello, G. Focardi, Direct Contact Condensation of Steam on Slowly Moving Water, *Nuclear Engineering and Design*, 1986, 96, 21–31

[14] M.H. Chun, Y.S. Kim, J.W. Park, An Investigation of Direct Condensation of Steam Jet in Subcooled Water, *International Communications in Heat and Mass Transfer*, 1996, 23(7), 947–958

[15] Y.S. Kim, and C.H. Song, Overall Review of Steam Jet Condensation in a Next Generation Reactor Water Pool, *Proceedings of IMECE'03*, ASME, 2003, 1–10

[16] Sherif, S.A., Lear, W.E., Steadham, J.M., Hunt, P.L., Holladay, J.B.: Analysis and Modeling of a Two-Phase Jet Pump of a Thermal Management System for Aerospace Applications, *International Journal of Mechanical Sciences*, 2000, 42, 185–198

[17] Beithou, N. & Aybar, H.S.: High-Pressure Steam-Driven Jet Pump-Part I: Mathematical Modeling, *Transactions of the ASME: Journal of Engineering for Gas Turbines and Power*, 2001, 123, 693–700

[18] The RELAP5 Code Development Team: *RELAP5/MOD3 Code Manual*, NUREG/CR-5535, Idaho National Engineering Laboratory, Idaho Falls, Idaho, USA, 1995

[19] Block, J.A.: Condensation-Driven Fluid Motions, *International Journal of Multiphase Flow*, 1980, 6, 113–129

[20] Aya, 1. & Nariai, H.: Boundaries Between Regimes of Pressure Oscillation Induced by Steam Condensation in Pressure Suppression Containment, *Nuclear Engineering and Design*, 1987, 99, 31–40

[21] Aya, 1. & Nariai, H.: Evaluation of Heat-Transfer Coefficient at Direct-Contact Condensation of Cold Water and Steam, *Nuclear Engineering and Design*, 1991, 131, 17–24

[22] Weimer, J.C., Faeth, G.M., Olson, D.R.: Penetration of Vapor Jets Submerged in Subcooled Liquids, *AIChE Journal*, 1973, 19(3), 552–558

[23] Petrovic - de With, A., Calay, R.K., de With, G.: Three Dimensional Condensation Regime Diagram for Direct Contact Condensation of Steam Injected into Water, *International Journal of Heat and Mass Transfer*, to be published in 2007

[24] Simpson, M.E. & Chan, C.K.: Hydrodynamics of a Subsonic Vapor Jet in Subcooled Liquid, *Journal of Heat Transfer*, 1982, 104, 271–278

[25] Petrovič — de With, A.: *Characterisation and Modelling of Flow Mechanisms for Direct Contact Condensation of Steam Injected into Water*, PhD thesis, University of Hertfordshire, UK, 2006

ACKNOWLEDGEMENTS

The photographs and some of the data presented in this paper are from experiments performed at Metafil AS, Norway and Det Norske Veritas, Norway. Authors thankfully acknowledge permission to use their experimental material.